

1 **3D printable conductive materials for the fabrication of electrochemical**
2 **sensors: A mini review**

3 **Hairul Hisham Hamzah^{1*}, Saiful Arifin Shafiee², Aya Abdalla^{3,4}, Bhavik Anil Patel^{3,4*}**
4

5 ¹School of Chemical Sciences, University of Science Malaysia (USM), 11800, Pulau Pinang, Malaysia

6 ²Chemistry, University of Southampton, University Road, Southampton, SO17 1BJ, UK

7 ³School of Pharmacy and Biomolecular Sciences, University of Brighton, Brighton, BN2 4GJ, UK

8 ⁴Centre for Stress and Age-Related Diseases, University of Brighton, Brighton, BN2 4GJ, UK
9

10 *Corresponding authors

11 E-mail address: hishamhamzah@usm.my

12 E-mail address: B.A.Patel@brighton.ac.uk
13
14
15

16 **Abstract**

17
18 The review presents recent developments in the use of conductive materials that can be
19 printed using additive manufacturing (3D printing), enabling the development of mass-
20 produced electrochemical sensors of varying geometries. This review will highlight some
21 key electroanalytical applications of 3D-printed electrochemical sensors and discuss their
22 potential future capabilities.
23

24 **Keywords:** 3D printing; additive manufacturing; electrochemistry; conductive electrode;
25 3D printed electrode; electrochemical sensor
26
27

28 **Contents**

- 29
30 1. Introduction
31 2. Conductive materials developed for 3D printing of electrodes
32 3. Electroanalytical applications of 3D printed electrodes
33 4. Conclusion and future work
34
-

35 **1. Introduction**

36
37 Three-dimensional (3D) printing technology, also known as additive manufacturing, has
38 been widely used to make complex devices and microfluidic channels which can be used
39 as platforms to house sensors made by conventional methods [1–6]. However, exploiting
40 the capabilities of 3D printing technology to fabricate materials that can function as
41 electroanalytical sensors has been a recent development, due to the availability of
42 conductive materials that can be used in printing [7–10].
43

44 The process of printing 3D objects usually starts by creating a model using computer-
45 aided design (CAD) software. This model must then be converted into the Standard
46 Triangle Language (STL) file format which stores information on the 3D object surfaces
47 as a list of coordinates of triangulated sections. This process is then followed by a slicing
48 procedure, where the 3D model is divided into several layers with 2D cross-sections,
49 which are then sent to a 3D printer to process. Finally, the 3D printer starts to deposit a
50 filament onto the print bed until the entire 3D object has been created. There are a number
51 of processes that can be used for 3D printing, which are detailed in a review by Ambrosi
52 and Pumera [7]. The most commonly used technique is a process of extrusion using fused
53 deposition modelling (FDM). This technique uses an additive approach, in which a
54 continuous thermoplastic filament is heated to a semi-molten state before extrusion for
55 layer-by-layer deposition [11,12]. This approach is simple and can be utilised to print
56 multi-material structures at low cost, which in turn provides high versatility. However, the
57 accuracy and surface quality can be relatively poor when compared to those of powder-
58 based plastic additive manufacturing processes [12].

59 3D printing of electrochemical sensors offers several interesting advantages over
60 conventional manufacturing methods as it can lower the production cost, provide rapid
61 prototyping, increase the manufacturing speed, and allow for the development of sensors
62 with complex geometries. Herein, we highlight the conductive materials that have been
63 used for the development of electrochemical sensors through 3D printing and their
64 applications.

65

66 **2. Conductive materials developed for 3D printing of electrodes**

67
68 Various materials have been employed for 3D printing in different sectors, in particular for
69 the development of electronic components [9,13,14] However very few studies have
70 transformed these materials into electrodes for sensing.

71
72 The majority of studies that have developed electrodes using 3D printing methods have
73 involved the printing of metals. In these studies, 3D stainless-steel electrodes were
74 printed and then electroplated with gold (Au) [15–20], bismuth (Bi) [20], nickel (Ni) [21],
75 platinum (Pt) [21] and iridium oxide (IrO₂) [21,22] to make electrodes suitable for a host
76 of analytical applications. However, printing of metal materials requires expensive
77 equipment and, in most cases, an additional fabrication step is required, where the
78 stainless-steel electrodes are electroplated with another metal to make the electrodes
79 suitable for sensing. Certain electrodeposited metals may also not be biocompatible or
80 suitable for environmental monitoring. Metal electrodes also offer a limited
81 electrochemical potential window, reducing their scope for use as sensors.

82 For these reasons, carbon-based materials are more attractive for the development of 3D
83 printed electrodes. To produce conductive carbon filaments, composite materials are
84 produced from conductive materials such as carbon nanotubes, graphene and carbon
85 black mixed with thermoplastic materials such as polylactic acid (PLA) and acrylonitrile
86 butadiene styrene (ABS). Printing of carbon composite filaments could offer significant
87 advantages in the development of conductive electrodes [23] when compared to carbon
88 paste and carbon nanotube-epoxy composite electrodes [24–26] as dispersion is better
89 regulated, providing enhanced batch-to-batch precision. However, the development of a
90 printable conductive filament is not a simple task, as an appropriate balance needs to be
91 struck between the fraction of conductive material that allows for a semi-molten state to
92 be achieved during printing, and appropriate conductivity of the printed electrode. At
93 present there are reports on conductive 3D printable polymer materials based on
94 PLA/graphene filaments [27–29], ABS/carbon black filaments [30,31],
95 polypropylene/carbon black filaments [9], polybutylene terephthalate/carbon
96 nanotube/graphene filaments [32] and carbon nanofiber/graphite/polystyrene composite
97 filaments [33,34].

98 Studies to date have shown that printing with carbon composite materials must be carried
99 out with care, as anisotropy and orientation of printing [30,31] can result in significant
100 variations in the electrochemical performance of the printed sensors, as shown in Figure
101 1 [31]. These studies highlight the importance of understanding the key parameters in
102 printing and their influence on the conductivity of composite electrodes, as these variables
103 can influence conductive pathways in composite materials.

104

105

Figure 1

106

107
108

109 **3. Electroanalytical applications of 3D printed electrodes**

110
111 There have been a host of electroanalytical applications using 3D printed electrodes,
112 among which we will highlight some key developments. Most of these applications have
113 employed metal printed devices developed by Pumera and colleagues [7,8], utilising a 3D
114 printed helical stainless-steel electrode, which was then electroplated with various metals
115 for sensing applications [15,17–20].

116 Using the stainless-steel helical template, gold films were electroplated to create a sensor
117 for the detection of single-stranded DNA (ssDNA). Using a self-assembled monolayer DNA
118 sensor, complementary ssDNA concentrations in the range 1 nM–1000 nM were detected
119 [15]. In a similar approach, 3D printed gold-plated electrodes were utilised for the detection
120 of phenol and *p*-aminophenol, where lower anodic potentials were observed when
121 compared to glassy carbon (GC) electrodes. However, the 3D printed electrodes only
122 showed higher sensitivity towards the detection of *p*-aminophenol, not phenol [17]. Gold
123 electroplated 3D metal electrodes were also shown to have enhanced sensitivity for the
124 determination of acetaminophen and dopamine when compared to GC and gold (Au) disk
125 electrodes [19]. To study heavy metal detection, thin films of Au and Bi were separately
126 electrodeposited on stainless-steel 3D printed electrodes. Figure 2 shows that both 3D
127 printed electrodes (3D-Au and 3D-Bi) showed higher sensitivities than a GC electrode for
128 the detection of lead (Pb) and cadmium (Cd). However, the limit of detection (LOD) values
129 for Pb and Cd obtained were higher than for the GC electrode [20]. Most recently, these
130 3D printed stainless-steel gold electroplated electrodes have been shown to be more
131 sensitive for the detection of 2,4,6-trinitrotoluene (TNT), 2,4-dinitrotoluene (DNT), and
132 fenitrothion (FT) than GC electrodes [18]. These studies all highlight the potential of 3D
133 printing of metal to make electrodes, but their electrochemical behavior was only achieved
134 through electroplating.

135

136

Figure 2

137

138 Carbon composites offer a more promising approach for the direct use of printed
139 conductive material. There are very few applications of carbon-based 3D printed electrodes
140 for sensing applications. An all polystyrene 3D printed electrochemical device with an
141 embedded carbon nanofiber/graphite/polystyrene composite electrode was shown to
142 provide excellent responses for the detection of Pb^{2+} via anodic stripping [33]. Using the
143 same electrode material, differential pulse anodic stripping voltammetry was used to
144 analyse Zn^{2+} in a sample of tap water [34]. An alternative approach for the detection of Cu^{2+}
145 cations was achieved using gold-coated 3D printed PLA/graphene electrodes with
146 immobilised cadmium sulfide nanoparticles present at the electrode surface as an active
147 semiconductor, where the LOD was lower than that obtained using indium tin
148 oxide/fluorine-doped tin oxide glass electrodes [29]. Most recently, a study used a
149 PLA/graphene filament to make 3D printed ring and disc electrodes for the detection of
150 picric and ascorbic acid. The electrodes, shown in Figure 3, demonstrated exceptional
151 linearity for measurement of picric acid (5 and 360 ppm) and ascorbic acid (10 and 500
152 ppm) [28]. These initial studies have shown that 3D printed conductive materials can
153 function as sensors and offer enhanced performance compared with commonly utilised
154 electrodes such as GC electrodes.

155

156

157

Figure 3

158

159

160

161 **4. Conclusion and Future work**

162

163 The availability of conductive materials suitable for 3D printing is likely to shape a new
164 wave of sensor development for electroanalytical applications. Carbon composite sensors
165 fabricated by 3D printing show enhanced precision when compared to carbon composite
166 electrodes produced by conventional approaches. To date, 3D printed metal or carbon
167 materials have been shown to have exceptional performance for the detection of metals
168 and organic compounds when compared to GC electrodes. The ability to make robust,
169 high-throughput, precisely fabricated electrodes using 3D printing technology provides a
170 new and attractive proposition for sensor development. However, there has still not been
171 enough comparison of 3D printed conductive materials with screen-printed electrodes or
172 other commonly used sensing materials. This is critical to understand the niche of these
173 sensing materials and future studies need to provide appropriate analytical comparison.

174

175 However, the use of 3D printing in the development of sensors is still in its infancy and
176 there is tremendous potential in the strategies that can be utilised for printing sensors and
177 in the exploration of geometries. As 3D printing occurs through the layer-by-layer
178 deposition of conductive materials, there is still plenty to explore in the most appropriate
179 printing parameters to ensure enhanced conductivity of the electrode material. Within
180 FDM, the print layer thickness, pattern of infill and printing orientation can all be altered
181 and therefore researchers have the opportunity to explore whether these parameters can
182 alter the electrochemical performance of carbon composite sensors. A study has already
183 shown that anisotropy and printing orientation can have a dramatic influence on the current
184 density and anodic peak potential of redox species [31].

185 One of the major advantages of 3D printing is the ability to create electrodes of different
186 geometries. At present all studies using 3D metal electrodes have been carried out using
187 helical [22] and gauze [21] shaped 3D printed devices, while carbon printed sensors have
188 mainly been rectangular [33] or disc electrodes [27–29,31]. With the ability to develop
189 complex geometries, the consequences of varying the shapes and sizes of electrodes
190 have yet to be explored. Due to limitations in fabricating different shapes, little is known
191 about how differently shaped electrodes behave in electrochemical sensing and we have

192 yet to explore more appropriate shapes to enhance electrode and mass transfer activity
193 for sensing. In this light, not only will 3D printing sensors be able to explore new analytes
194 for measurement but there may also be new applications where sensors can be shaped
195 to suit specific applications where conventional geometries do not perform well.

196 Finally, there is plenty of potential for the development of conductive materials for 3D
197 printing. At present the range of 3D printed conductive materials is limited and, particularly
198 in the case of composite conductive filaments, there is scope for the development of more
199 interesting conductive materials that can increase the array of analytes that can be
200 monitored. In the future, conductive carbon filaments may also have additional chemical
201 modifiers or mediators that allow for specific tailoring of the printed conductive material
202 for electrocatalytic reactions or to serve as base electrodes for biosensors. More complex
203 filaments consisting of a mixture of conductive materials and polymers for specialized
204 sensing applications are also likely to be developed.

205 In summary, conductive materials that can be used to fabricate electrodes using 3D
206 printing have been developed and show significant promise. This is only the tip of the
207 iceberg, however, as there is tremendous potential in the conductive materials that can
208 be printed and the geometries that can be produced, opening up new avenues for
209 electroanalytical sensing.

210 **Total words (Abstract to Section 4 = 1925 words)**

211 **Conflict of interest statement**

212
213 The authors declare no conflict of interest.

214
215
216 **Acknowledgement**

217
218 The authors would like to thank the University of Science Malaysia (USM) for the financial
219 support to cover the publication fee.

220

221

222 **References**

223 [1] M.D. Symes, P.J. Kitson, J. Yan, C.J. Richmond, G.J.T. Cooper, R.W. Bowman, T.
224 Vilbrandt, L. Cronin, Integrated 3D-printed reactionware for chemical synthesis and
225 analysis, *Nat. Chem.* 4 (2012) 349–354.

226 [2] Q. Sun, J. Wang, M. Tang, L. Huang, Z. Zhang, C. Liu, X. Lu, K.W. Hunter, G. Chen,
227 A new electrochemical system based on a flow-field shaped solid electrode and 3D-
228 printed thin-layer flow cell: detection of Pb²⁺ ions by continuous flow accumulation
229 square-wave anodic stripping voltammetry, *Anal. Chem.* 89 (2017) 5024–5029.

230 [3] J.L. Erkal, A. Selimovic, B.C. Gross, S.Y. Lockwood, E.L. Walton, S. McNamara, R.S.
231 Martin, D.M. Spence, 3D printed microfluidic devices with integrated versatile and
232 reusable electrodes, *Lab Chip.* 14 (2014) 2023–2032.

233 [4] M. Banna, K. Bera, R. Sochol, L. Lin, H. Najjaran, R. Sadiq, M. Hoorfar, M. Banna, K.
234 Bera, R. Sochol, L. Lin, H. Najjaran, R. Sadiq, M. Hoorfar, 3D printing-based
235 integrated water quality sensing system, *Sensors* 17 (2017) 1336.

236 [5] A.S. Munshi, R.S. Martin, Microchip-based electrochemical detection using a 3-D
237 printed wall-jet electrode device, *Analyst* 141 (2016) 862–869.

238 [6] G.W. Bishop, J.E. Satterwhite, S. Bhakta, K. Kadimisetty, K.M. Gillette, E. Chen, J.F.
239 Rusling, 3D-Printed fluidic devices for nanoparticle preparation and flow-injection
240 amperometry using integrated prussian blue nanoparticle-modified electrodes, *Anal.*
241 *Chem.* 87 (2015) 5437–5433.

242 [7] A. Ambrosi, M. Pumera, J. Yan, C.J. Richmond, G.J.T. Cooper, R.W. Bowman, T.
243 Vilbrandt, L. Cronin, R. Mülhaupt, R. Polsky, R.J. Narayan, J.M. DeSimone, 3D-
244 printing technologies for electrochemical applications, *Chem. Soc. Rev.* 45 (2016)
245 2740–2755.

246 [8] C.L. Manzanares Palenzuela, M. Pumera, (Bio)analytical chemistry enabled by 3D
247 printing: sensors and biosensors, *TrAC Trends Anal. Chem.* 103 (2018) 110–118.

- 248 [9] S.W. Kwok, K.H.H. Goh, Z.D. Tan, S.T.M. Tan, W.W. Tjiu, J.Y. Soh, Z.J.G. Ng, Y.Z.
249 Chan, H.K. Hui, K.E.J. Goh, Electrically conductive filament for 3D-printed circuits and
250 sensors, *Appl. Mater. Today* 9 (2017) 167–175.
- 251 [10] M. Pohanka, Three-dimensional printing in analytical chemistry: principles and
252 applications, *Anal. Lett.* 49 (2016) 2865–2882.
- 253 [11] S.S. Crump, Apparatus and method for creating three-dimensional objects, in *Google*
254 *Patents*, 1992.
- 255 [12] H. Bikas, P. Stavropoulos, G. Chryssolouris, Additive manufacturing methods and
256 modelling approaches: a critical review, *Int. J. Adv. Manuf. Technol.* 83 (2016) 389–
257 405.
- 258 [13] J.-Y. Lee, J. An, C.K. Chua, Fundamentals and applications of 3D printing for novel
259 materials, *Appl. Mater. Today* 7 (2017) 120–133.
- 260 [14] S.J. Leigh, R.J. Bradley, C.P. Purcell, D.R. Billson, D.A. Hutchins, A simple, low-cost
261 conductive composite material for 3D printing of electronic sensors, *PLoS One* 7
262 (2012) e49365.
- 263 [15] A.H. Loo, C.K. Chua, M. Pumera, DNA biosensing with 3D printing technology,
264 *Analyst* 142 (2017) 279–283.
- 265 [16] E.H.Z. Ho, A. Ambrosi, M. Pumera, Additive manufacturing of electrochemical
266 interfaces: simultaneous detection of biomarkers, *Appl. Mater. Today* 12 (2018) 43–
267 50.
- 268 [17] T.S. Cheng, M.Z.M. Nasir, A. Ambrosi, M. Pumera, 3D-printed metal electrodes for
269 electrochemical detection of phenols, *Appl. Mater. Today* 9 (2017) 212–219.
- 270 [18] C. Tan, M.Z.M. Nasir, A. Ambrosi, M. Pumera, 3D printed electrodes for detection of
271 nitroaromatic explosives and nerve agents, *Anal. Chem.* 89 (2017) 8995–9001.
- 272 [19] B.R. Liyarita, A. Ambrosi, M. Pumera, 3D-printed electrodes for sensing of biologically
273 active molecules, *Electroanalysis* 30 (2018) 1319–1326.
- 274 [20] K.Y. Lee, A. Ambrosi, M. Pumera, 3D-printed metal electrodes for heavy metals
275 detection by anodic stripping voltammetry, *Electroanalysis* 29 (2017) 2444–2453.
- 276 [21] A. Ambrosi, M. Pumera, Self-contained polymer/metal 3D printed electrochemical
277 platform for tailored water splitting, *Adv. Funct. Mater.* 28 (2018) 1700655.
- 278 [22] A. Ambrosi, J.G.S. Moo, M. Pumera, Helical 3D-printed metal electrodes as custom-
279 shaped 3D platform for electrochemical devices, *Adv. Funct. Mater.* 26 (2016) 698–
280 703.
- 281 [23] N. Patel, A. Fagan-Murphy, D. Covill, B.A. Patel, 3D printed molds encompassing
282 carbon composite electrodes to conduct multisite monitoring in the entire colon, *Anal.*
283 *Chem.* 89 (2017) 11690–11696.

- 284 [24] A. Fagan-Murphy, S. Kataria, B.A. Patel, Electrochemical performance of multi-walled
285 carbon nanotube composite electrodes is enhanced with larger diameters and
286 reduced specific surface area, *J. Solid State Electrochem.* 20 (2016) 785–792.
- 287 [25] A. Fagan-Murphy, B.A. Patel, Compressed multiwall carbon nanotube composite
288 electrodes provide enhanced electroanalytical performance for determination of
289 serotonin, *Electrochim. Acta* 138 (2014) 392–399.
- 290 [26] M. Pumera, A. Merkoçi, S. Alegret, Carbon nanotube-epoxy composites for
291 electrochemical sensing, *Sensors Actuators B Chem.* 113 (2006) 617–622.
- 292 [27] C.W. Foster, M.P. Down, Y. Zhang, X. Ji, S.J. Rowley-Neale, G.C. Smith, P.J. Kelly,
293 C.E. Banks, 3D printed graphene based energy storage devices, *Sci. Rep.* 7 (2017)
294 42233.
- 295 [28] C.L. Manzanares Palenzuela, F. Novotný, P. Krupička, Z. Sofer, M. Pumera, 3D-
296 printed graphene/polylactic acid electrodes promise high sensitivity in electroanalysis,
297 *Anal. Chem.* 90 (2018) 5753–5757.
- 298 [29] C.Y. Foo, H.N. Lim, M.A. Mahdi, M.H. Wahid, N.M. Huang, Three-dimensional printed
299 electrode and its novel applications in electronic devices, *Sci. Rep.* 8 (2018) 7399.
- 300 [30] J. Zhang, B. Yang, F. Fu, F. You, X. Dong, M. Dai, Resistivity and its anisotropy
301 characterization of 3D-printed acrylonitrile butadiene styrene copolymer (ABS)/carbon
302 black (CB) composites, *Appl. Sci.* 7 (2017) 20.
- 303 [31] H.H. Bin Hamzah, O. Keattch, D. Covill, B.A. Patel, The effects of printing orientation
304 on the electrochemical behaviour of 3D printed acrylonitrile butadiene styrene
305 (ABS)/carbon black electrodes, *Sci. Rep.* 8 (2018) 9135.
- 306 [32] K. Gnanasekaran, T. Heijmans, S. van Bennekom, H. Woldhuis, S. Wijnia, G. de With,
307 H. Friedrich, 3D printing of CNT- and graphene-based conductive polymer
308 nanocomposites by fused deposition modeling, *Appl. Mater. Today* 9 (2017) 21–28.
- 309 [33] Z. Rymanšaub, P. Iravani, E. Emslie, M. Medvidović-Kosanović, M. Sak-Bosnar, R.
310 Verdejo, F. Marken, All-polystyrene 3D-printed electrochemical device with embedded
311 carbon nanofiber-graphite-polystyrene composite conductor, *Electroanalysis* 28
312 (2016) 1517–1523.
- 313 [34] K.C. Honeychurch, Z. Rymanšaub, P. Iravani, Anodic stripping voltammetric
314 determination of zinc at a 3-D printed carbon nanofiber–graphite–polystyrene
315 electrode using a carbon pseudo-reference electrode, *Sensors Actuators B Chem.*
316 267 (2018) 476–482.

317

318

Figures

Figure 1. 3D printed electrodes. (A) shows the approach in which the horizontal and vertical print of the ABS/carbon black material was used to generate vertical printed (VP), horizontal printed smooth surface (HPSS) and horizontal printed rough surface (HPRS) electrodes. The cross-section of the electrode is shown on the right. (B) Photographs of 3D printed carbon black/ABS electrodes showing electrodes printed vertically and horizontally. (C) Cyclic voltammograms of glassy carbon (GC), VP, HPRS and HPSS for 1 mM ferrocene carboxylic acid in 0.1 M NaOH measured at a scan rate of 100 mV/s. Responses of (D) anodic peak current normalised to electrode surface area (i_{pa}) and (E) anodic peak potential (E_{pa}) for 1 mM ferrocene carboxylic acid. Statistical analyses were performed using one-way ANOVA followed by a post hoc Tukey test. Data are shown as mean \pm S.D., $n=4$, * $P < 0.05$, ** $P < 0.01$ and *** $P < 0.001$. Adapted and reprinted with permission from ref 23. Copyright (2018) Nature Publishing Group

Figure 2. (A) Schematic of the electrode design as obtained by CAD software. Photographs of 3D-printed electrodes (B) as printed (3D-steel), (C) after electroplating with Au (3D-Au) and (D) after electroplating with Bi (3D-Bi). Scale bar corresponds to 1 cm. Square-wave stripping voltammograms for increasing concentrations of Pb in 50 ppb steps for (E) GC, (F) 3D-steel, (G) 3D-Au and (H) 3D-Bi electrodes, with a concentration range of 50–300 ppb. Also shown are the corresponding blank voltammograms (black lines). Experimental conditions: deposition potential of -1.3 V for 120 s, scans with frequency of 25 Hz, potential step of 4 mV and amplitude of 25 mV. 0.1 M acetate buffer (pH 4.5) was used as supporting electrolyte. Adapted and reprinted with permission from ref 13. Copyright (2018) Wiley-VCH

Figure 3. (A) 3D-printed electrode dimensions and shapes. Cyclic voltammograms of 3D-printed graphene electrodes recorded for different concentration levels of (B) picric acid in acetate buffer 0.1 M pH 4.6 (inset: calibration plot using anodic peak intensity) and (C) ascorbic acid in KCl 0.1 M (inset: calibration plot). Dashed line: nonactivated electrodes in the presence of the highest concentration of analyte. Discontinuous line: blank current in the supporting electrolyte. Full lines from light gray to black: activated electrodes in the presence of increasing analyte level (5 to 360 ppm for picric acid and 10 to 500 μ M for ascorbic acid). Adapted and reprinted with permission from ref 21. Copyright (2018) American Chemical Society.

Figure 1

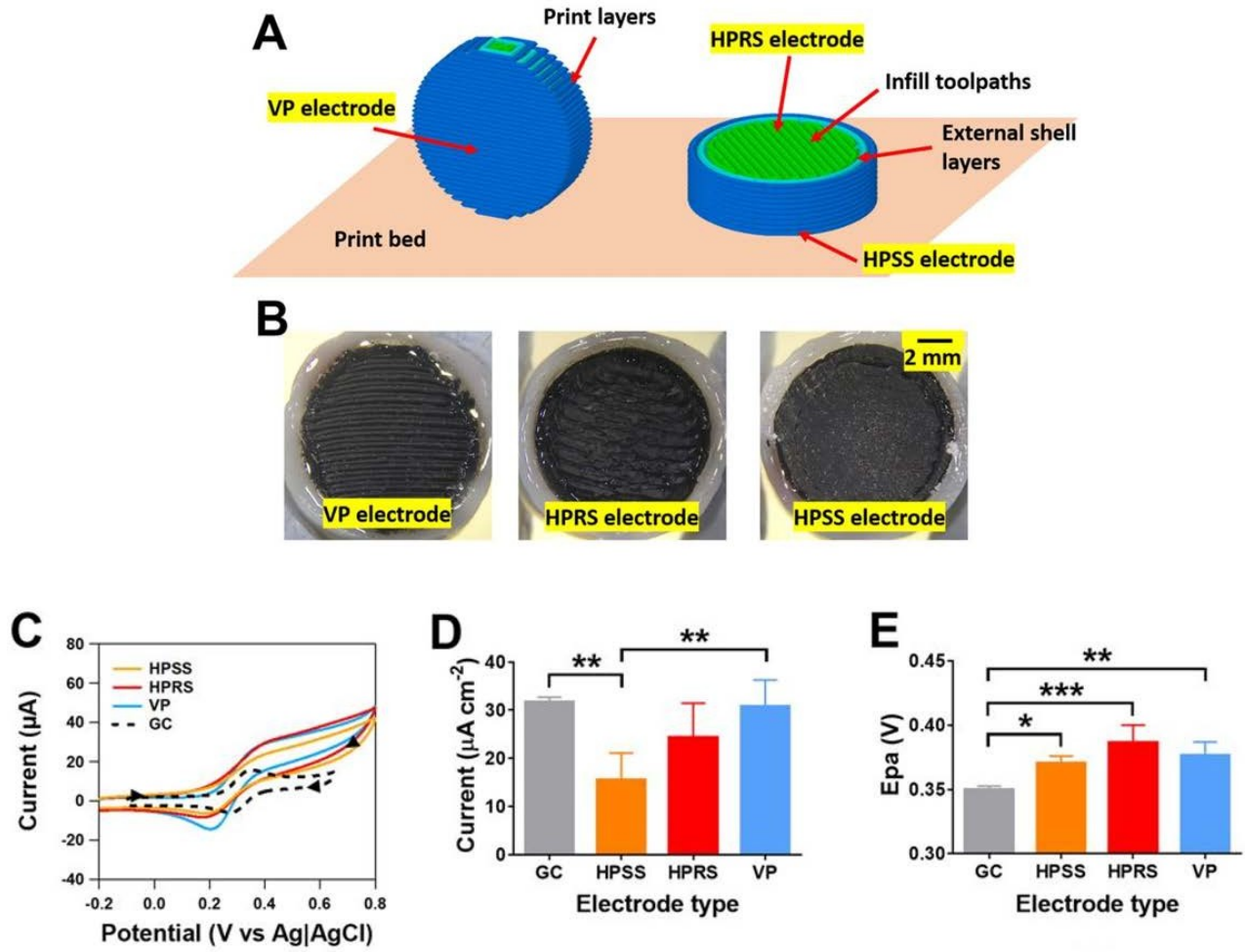


Figure 2

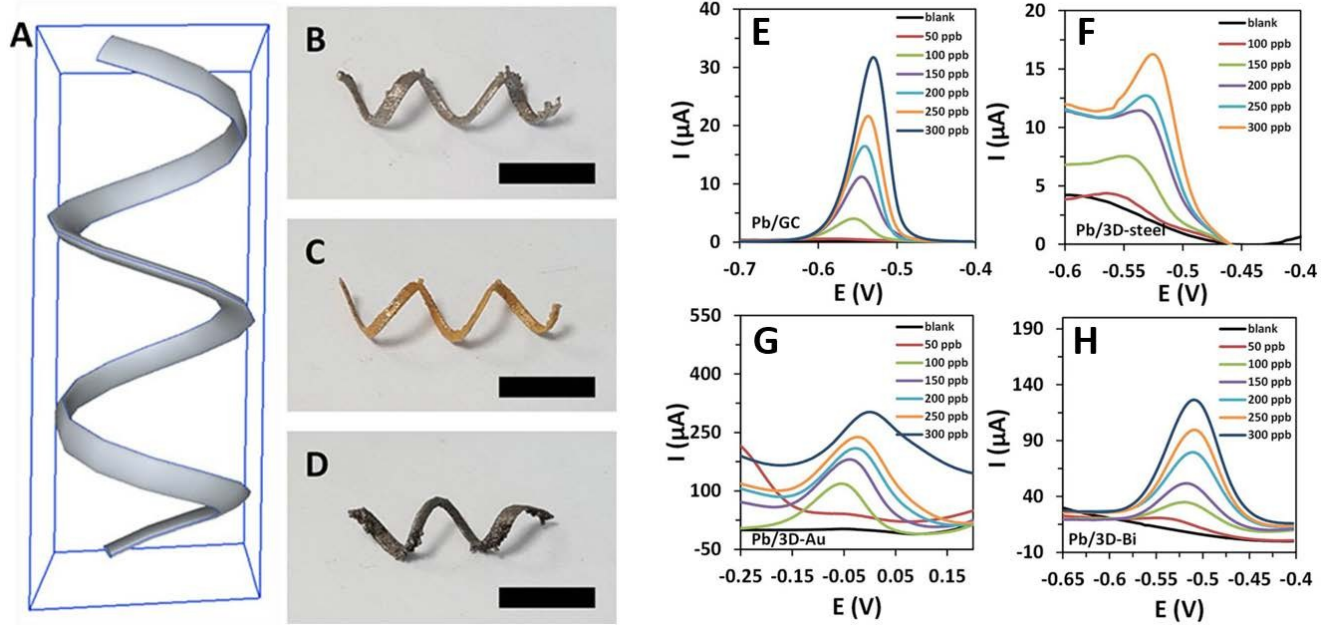


Figure 3

